CrossMark

Hydrothermal synthesis of carbon dots codoped with nitrogen and phosphorus as a turn-on fluorescent probe for cadmium(II)

Liping Lin[1] · Yuhan Wang[1] · Yanling Xiao[1] · Wei Liu[2]

Abstract

Nitrogen and phosphorus co-doped carbon dots (N,P-CDs) have been synthesized via hydrothermal method starting from o-phosphorylethanolamine and citric acid. The blue-green fluorescence of the N,P-CDs (with excitation/emission peaks at 325/435 nm) is gradually enhanced on sequential addition of Cd(II) ions. This fluorometric assay works in the 0.5 μM to 12.5 μM Cd(II) concentration range and has a 0.16 μM detection limit. The phenomenon may be attributed to chelation enhanced fluorescence that is induced by the formation of Cd(II)-N,P-CDs complex with functional groups present on the surface. The method has applied to the detection of Cd(II) in spiked serum and urine samples and gave satisfying results.

Introduction

Cd(II) has been extensively utilized in industry and agriculture. However, according to the classification of the Agency for Toxic Substances, Disease Registry and U.S. Environmental Protection Agency (EPA), Cd(II) comes in seventh on the Top 20 Hazardous Substances Priority List [1]. Long-term exposure to Cd(II) has caused a series of serious environmental and health problems, including pneumonitis, pulmonary edema, emphysema and even some cancers [2]. Therefore, it is of considerable significance to develop sensitive and selective methods for the detection of Cd(II) for human health and environmental conservation. Up to now, fluorescent methods have been mostly adapted due to their high selectivity and sensitivity, micro samples and low cost [3–6]. However, plentiful of fluorescent organic materials and metal-

based nanomaterials used in the fluorescent methods would cause newly environmental issue. Furthermore, most of them adopt fluorescence quenching and "off-on" detection mode, which reduce the detection sensitivity and complicate the detection procedure [4, 5, 7].

As a novel alternative to fluorescent organic materials and metal-based nanomaterials, fluorescent carbon dots (CDs) have aroused much attention due to their excellent optical properties, low toxicity, good bio-compatibility and favourable water solubility [8, 9]. However, the generally low quantum yield (QY) and few active sites of CDs have been limited their wider applications in ions and molecules detection, bio-imaging, photo-catalysis and so on [10, 11]. Heteroatom doping has been proved to be an effective strategy to enhance the QY of CDs and provide available sites for target sensing in biological and environmental fields [10, 11]. As is known, nitrogen endows comparable atomic size to carbon and five valence electrons [12], and phosphorus can form substitution defect in sp^3-bonded diamond thin films as it plays as an n-type donor [13]. It is believed that the doping of nitrogen and phosphorus into CDs would alter electronic characteristics of CDs and effectively modulate their physicochemical properties. Therefore, the methods including solid phase synthesis [14], microwave-assisted methods [15], combining carbonization with subsequent chemical exfoliation [16] and hydrothermal methods [17–19] have been reported for the synthesis of nitrogen and phosphorus co-doped CDs (N,P-CDs). As a result, the N,P-CDs exhibited higher QY,

✉ Liping Lin
linliping2015@fafu.edu.cn

1 Department of Applied Chemistry, College of Life Sciences, Fujian Agriculture and Forestry University, Fuzhou 350002, China

2 Department of Bioinformatics, College of Life Sciences, Fujian Agriculture and Forestry University, Fuzhou 350002, China

more active sites, and even introduction of new and unanticipated properties [14, 20, 21].

Among these available synthesis approaches, hydrothermal methods have been widely adopted due to their relatively mild reaction conditions. Therefore, hydrothermal method has been adopted to synthesize N,P-CDs with o-phosphorylethanolamine (PEA) and citric acid (CA) as sources. The N,P-CDs with blue-green emission and high QY of 8.17% display excitation-dependent emission and excellent stability in both high-salt conditions and different pH values. Moreover, we were pleased to find that the N,P-CDs respond to Cd(II) by giving a fluorescence enhancement (Scheme 1). The mechanism studies indicate that the fluorescence enhancement in the presence of Cd(II) is attributed to the chelation enhanced fluorescence via the coordination reaction between the functional groups on the surface and Cd(II). This turn-on fluorescence probe is selective and sensitive to Cd(II) in the range of 0.5–12.5 μM with a detection limit of 0.16 μM. The probe is also suitable for Cd(II) analysis in real water samples.

Experimental

Reagents and chemicals

O-phosphorylethanolamine (PEA) was purchased from Sigma-Aldrich (USA, https://www.sigmaaldrich.com/catalog/product/sial/73104?lang=zh&region=CN). Citric acid (CA), acetic acid (HAc) and sodium acetate (NaAc) were obtained from Sinopharm Chemical Reagent Co., Ltd. (Shanghai, China, http://www.sinoreagent.com/). Cadmium chloride was from Zhanyun Chemical Co., Ltd. (Shanghai, China, http://www.shzychem.com/product.html). Cation stock solutions used in this experiment were prepared from their chloride or nitrate salts. All the chemicals were of analytical grade and used without any pretreatment. Cellulose membrane dialysis bag (retained molecular weight: 1000 Da) was purchased from Sangon Biotech Co., Ltd. (Shanghai, China, http://www.sangon.com/). Ultrapure water (18.2 MΩ) from a Laboratory Ultrapure Water System (Kertone Water Treatment Co., Ltd., China) was used throughout the whole experiments.
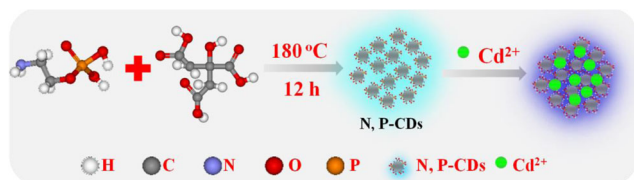
Scheme 1 Schematic presentation of the synthesis of N,P-CDs and their application as a turn-on fluorescent probe for Cd(II) detection

Characterization

Absorption spectra were obtained on a UV2600 spectrophotometer (Shimadzu, China) with a 1 cm quartz cell. Fourier transform-infrared (FT-IR) spectra were recorded using a Nicolet AVATAR 360 spectrophotometer (ThermoElectron Corp., USA) with the KBr pellet technique in the range of $400–4000\ cm^{-1}$. Fluorescence spectra and quantum yield were measured using a FLS 980 spectrofluorimeter (Edinburgh Instrument, UK). X-ray photoelectron spectroscope (XPS) spectra were measured at an X-ray photoelectron spectrometer (ESCALAB 250Xi, Thermo Fischer, USA). Transmission electron microscopy (TEM) images were performed on a JEM-2100F (JEOL, Japan) transmission electron microscope operated at an acceleration voltage of 200 kV. X-ray diffraction (XRD) patterns were measured on a Rigaku Ultima IV X-ray diffractometer with Cu Kα radiation (40 kV, 20 mA, λ = 1.54051 Å) (Kuraray Co., Ltd., Japan).

Synthesis of N,P-CDs

In a typical procedure, 0.5 mmol CA and 0.5 mmol PEA were mixed with 75 mL water in a Teflon-lined autoclave, and the mixture was heated at 180 °C for 12 h. After cooling to room temperature, Na_2CO_3 power was added to the yellow solution to neutralize the pH to 7.0. Then, the solution was subjected into a dialysis bag overnight to completely remove salt ions. After dialysis, the solution was filtered through 0.22 μm membrane filter to remove the precipitate. Finally, the N,P-CDs was lyophilized and re-dissolved into 100 mL with ultrapure water, and stored at 4 °C for future use.

Detection of Cd²⁺ with N,P-CDs

Different concentrations of Cd^{2+} were added into the mixture of 200 μL N,P-CDs and 100 μL acetate buffer (10 mM, pH 6.0), and then diluted to 2 mL with ultrapure water. After reacting at room temperature for 15 min, the fluorescence intensity was measured at an FLS 980 spectrofluorimeter with excitation/emission peaks at 325/435 nm.

Pre-treatment of real samples

Human serum samples and urine samples were obtained from healthy adult volunteers at Fujian Agriculture and Forestry University infirmary. 10 mL serum samples and urine samples were taken out and centrifuged at 8000 rpm for 20 min to eliminate the insoluble substance, respectively. Then, the supernatant was filtered with 0.22 μm membrane filter, and the filter were diluted 100-fold with ultrapure water as stock solution for further analysis.

Results and discussion

Choice of materials

Up to now, the mostly used nitrogen and phosphorus sources are adenosine-5′-triphosphate (ATP) [16, 22], the mixture of ethylenediamine and H_3PO_4 [17, 23] or organic phosphorus compounds [19], diammonium hydrogen phosphate [24], the mixture of ammonium hydroxide and H_3PO_4 [18] and few natural products [25, 26]. These nitrogen and phosphorus sources are relatively monotonous. Some of them are even harmful and need to control temperature to avoid any potential explosion [24]. As an environmentally friendly reagent, PEA plays an important role in the metabolism of phospholipid. The amino group and phosphate group in its backbone structure increase the possibility of the formation of complexes with metal ions. Therefore, PEA is used as nitrogen and phosphorus source in this work.

Characterizations of N,P-CDs

The N,P-CDs were highly stable at room temperature for nearly two months without any obvious aggregation (Fig. S1). They were nearly spherical in shape and uniformly dispersed (Fig. 1a). The high resolution TEM image displayed that there was an obvious highly crystalline structure with a lattice distance of ca. 0.24 nm (top inset in Fig. 1a), which is comparable to the (001) facet of graphite [19]. Taking 50 particles into account, the diameter distribution was in the range of 1.0–2.0 nm with an average diameter of 1.6 nm (lower inset in Fig. 1a), which is consistent with that of the N,P-CDs prepared with ATP [22].

XPS measurements shown that there were C1s, N1 s, P2p and O1s appeared at 285.4, 402.4, 133.4 and 531.4 eV with the relative element contents of approximately 56.59% (C), 7.13% (N), 28.64% (O) and 7.64% (P), respectively (Fig. 1b), which indicated the successful introduction of both nitrogen and phosphorus atoms. The high resolution C1s spectrum (**Fig. S2a**) was disassembled into three peaks attributed to C-C/C=C (284.4 eV), C-P=O/C-N (285.7 eV) and C=O/C=N (287.9 eV), respectively [18]. And there were C=O (530.7 eV), C-OH/P-O (531.7 eV) and O=C-OH (531.8 eV) exhibited in O1s spectrum (**Fig. S2b**) [27]. The N1 s spectrum presented C-N-C (399.2 eV), N-H (399.8 eV) and N-N/P-N (401.5 eV) (**Fig. S2c**) [23]. The P2p spectrum (**Fig. S2d**) was fitted to P-O (130.9 eV) and P-C/P-N (134.1 eV) [25].

On the other hand, as shown in FITR spectrum (Fig. 1c), there was stretching vibration peak located at 3430 cm^{-1} ascribed to –OH/–NH_2 group. The sharp absorption peaks at 1673 cm^{-1}, 1588 cm^{-1} and 1406 cm^{-1} were assigned to the stretching vibration of C=O band, C=N bond and –CH_3 group, respectively [28]. The characteristic peaks located at 540 cm^{-1}, 970 cm^{-1}, 1069 cm^{-1} and 1155 cm^{-1} were attributed to PO_4^{3-}, P-O-H, P-O-C and P=O, respectively [18, 23, 28]. All these results also proved the successful doping of nitrogen and phosphorus atoms in N,P-CDs. These results also indicated that there were many functional groups such as -COOH, -OH, -NH_2 and -PO_4^{3-} on the surface of N,P-CDs, which were conducive to the high hydrophilicity and stability in aqueous solution.

Optical properties

The N,P-CDs solution was pale yellow in daylight and exhibited blue-green under irradiation of 365 nm UV light (Inset in Fig. 1d). The UV-Vis spectrum displayed that there was a peak located at 325 nm (Fig. 1d), which was attributed to n-π* transitions of the sp^2 clusters [14]. Furthermore, the effects of (a) excitation wavelength, (b) NaCl concentration and (c) sample pH values on the optical behaviour have also been carried out. Results show that emission wavelength was excitation-dependent with the excitation wavelength ranging from 275 nm to 345 nm (**Fig. S3a**), and the emission intensity reached the maximum at 435 nm when the excitation wavelength was 325 nm. The QY was measured to be 8.17% with quinine sulphate in 0.1 M H_2SO_4 (QY = 0.58) as a reference, which was higher or comparable to those in previous work [14, 28]. Additionally, there was only slight fluorescence intensity change of in the presence of different concentrations of NaCl (0–1.0 M) (**Fig. S3b**) and pH values (2–11) (**Fig. S3c**). These results promise the feasible applications of N,P-CDs under high ionic strength conditions and physiological conditions.

Detection mechanism of Cd(II) with N,P-CDs as a turn-on fluorescent probe

The fluorescence of N,P-CDs is gradually enhanced on sequential titration with Cd(II). This demonstrates that they can be applied as a turn-on fluorescent probe for Cd(II) detection. As the concentration of Cd(II) increased from 0.5 μM to 32.5 μM, the fluorescence intensity of N,P-CDs gradually enhanced with the emission wavelength slightly blue-shifting from 435 nm to 427 nm (Fig. 2a) and reached the maximum and kept almost constant upon the addition of 20 μM Cd(II) (Fig. 2b).

Though the origin and mechanism for the photoluminescence of CDs are still ambiguous, it is widely accepted that the fluorescence emission of CDs was arose from the radioactive combination of the trapped surface holes and electrons on their surface [29]. Previous studies employ CDs to detect metal ions based on the coordination between the functional groups on the surface of CDs and metal ions
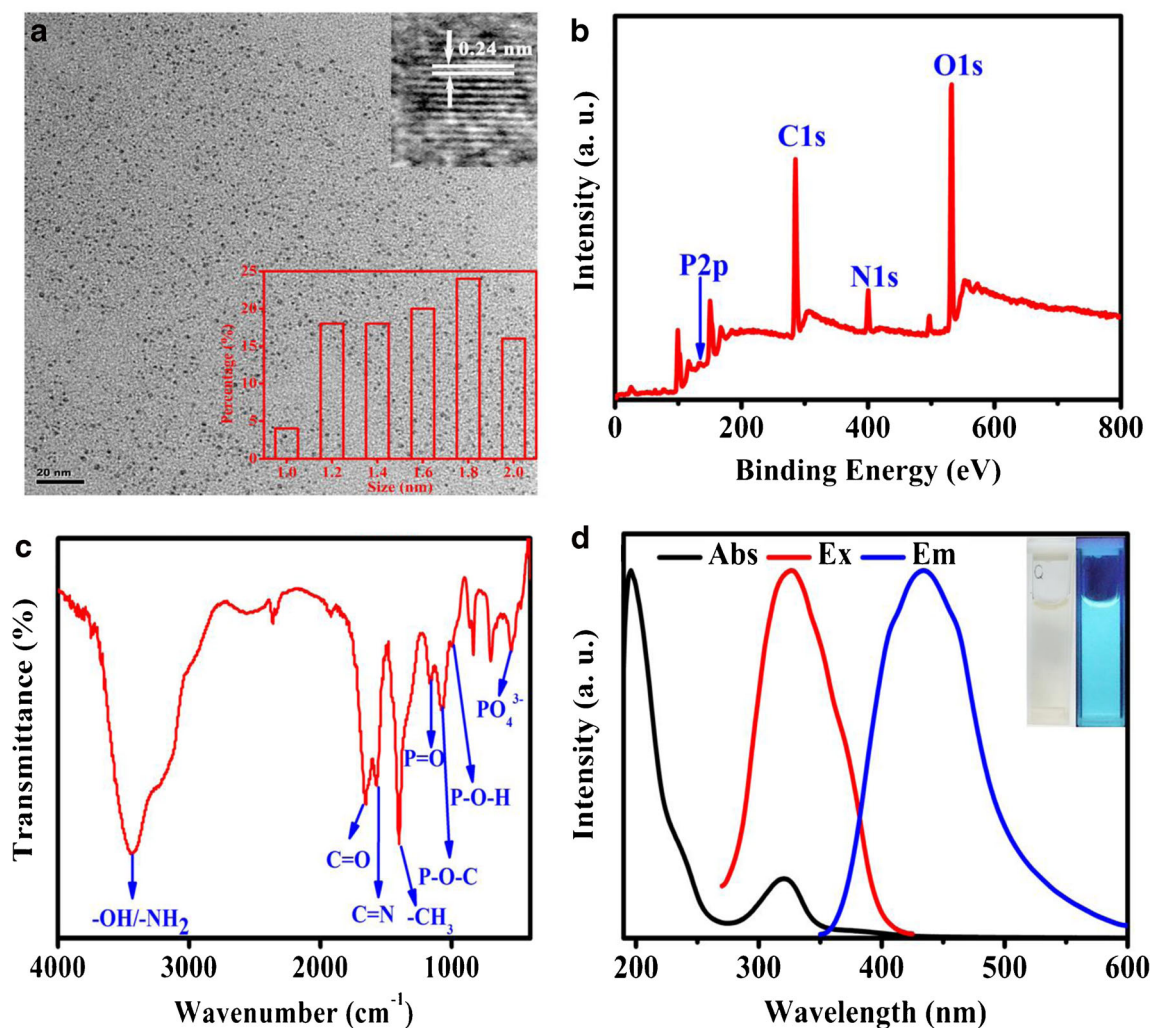
Fig. 1 **a** Typical TEM image of N,P-CDs (top inset: HRTEM image of an individual N,P-CDs nanoparticle; lower inset: diameter size distribution histogram by taking 50 particles into account.); **b** XPS survey spectrum; **c** FTIR spectrums; **d** Normalized UV-Vis absorption spectrum and fluorescence spectrums (Inset: Photographs of N,P-CDs under the radiation of (left) visible light and (right) 365 nm UV light)
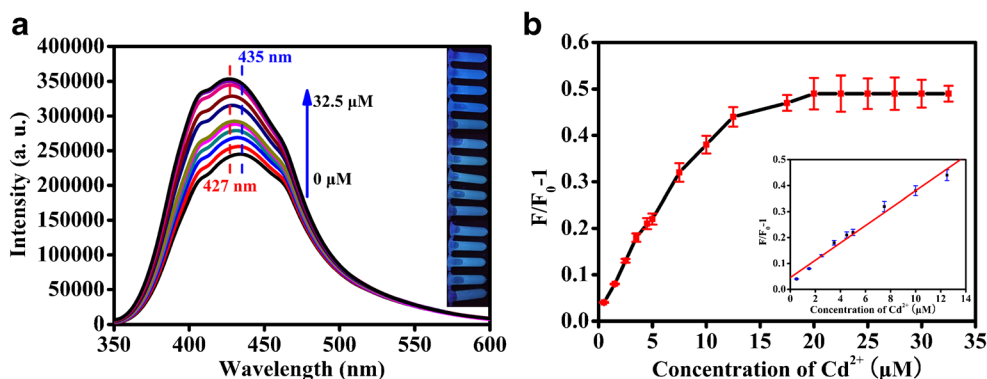

Fig. 2 **a** Emission spectra of N,P-CDs with various concentrations of Cd(II) in 10 mM pH 6.0 HAc-NaAc buffer (Inset: Photographs of N,P-CDs with various concentrations of Cd(II) under a 365 nm UV lamp.); **b** Relationship between fluorescence intensity variation and Cd(II) concentration ranging from 0.5 μM to 32.5 μM (Inset: The linear relationship between fluorescence intensity variation and Cd(II) concentration in the range 0.5–12.5 μM.). Experimental conditions: The total 2 mL of solution containing 200 μL N,P-CDs, different concentrations of Cd(II) and 100 μL HAc-NaAc (10 mM, pH 6.0) reacted for 15 min at room temperature. Each point is an average of three successive measurements. Error bars represent the standard error derived from three successive measurements

[7–9]. According to the acid-base theory, Cd(II), known as a "hard" acid similar to Al^{3+} [30], preferentially chelated with "hard" base groups presented on the surface of N,P-CDs. The oxygen atom in the –COOH, -OH, $-PO_4^{3-}$ and the nitrogen atom in the $-NH_2$ of N,P-CDs coordinated to Cd(II), forming a stable Cd(II)-N,P-CDs complex by providing lone pairs into empty orbitals of Cd(II) [31]. As a result, the fluorescence is enhanced.

To confirm the formation of Cd(II)-N,P-CDs complexes, several characterizations of N,P-CDs with and without Cd(II) were carried out. As shown in **Fig. S4a**, the average diameter size of N,P-CDs was 3.0 nm in the presence of Cd(II), which was larger than that of 1.6 nm in the absence of Cd(II) (Fig. 1a). The Zeta-potential increased from −15.6 eV to −10.1 eV after the addition of 5 μM Cd(II) (**Fig. S4b**), indicating that the negative charges of N,P-CDs has been partially neutralized by Cd(II) with positive charges via electrostatic action. Furthermore, FTIR spectra showed that the intensity of functional groups gradually decreased with increasing addition of Cd(II), and the $-PO_4^{3-}$ groups even disappeared in the presence of Cd(II) (Fig. 3a). All the above results proved the formation of Cd(II)-N,P-CDs complexes.

Generally, metal-enhanced fluorescence mechanism is generally divided into surface plasmon enhanced fluorescence (SPEF) and chelation enhanced fluorescence (CHEF) [32]. Since there was no obvious change observed in the UV-Vis absorption spectra of N,P-CDs with and without Cd(II) (**Fig. S4c**), the SPEF mechanism was eliminated [33]. On the other hand, it has been reported that the chelation between surface functional groups and metal ions would decrease intramolecular electron transfer, improve photoinduced electron transfer and enhance the emission [32]. The fluorescence enhancement may be the result of photoinduced electron transfer [34] assigned to the formation of Cd(II)-N,P-CDs complexes. That is, CHEF is likely the main mechanism for the fluorescence enhancement.

Analytical performances of the turn-on fluorescence probe for Cd(II) detection

To obtain excellent analytical performances, the optimization of (a) sample pH value and (b) incubation time was implemented. As shown in **Fig. S5**, the best experimental conditions were found when the Cd(II) detection was carried out in the sample pH value of 6 after incubating with N,P-CDs for 15 min. Under the optimum experimental conditions, the fluorescence intensity change was in an excellent linear relationship with the concentration of Cd(II) in the range of 0.5–12.5 μM. The linear equation was $F/F_0 – 1 = 0.04564 + 0.03346 C_{Cd(II)}$ with a linear correlation (R) of 0.9917. Here, F and F_0 were the fluorescence in the presence of and in the absence of Cd(II), respectively. The resulting detection limit of Cd(II) was 0.16 μM based on a signal-to-noise ratio of 3, which was comparable to previous work (**Table S1**).

To evaluate the selectivity of the response to Cd(II), several common metal ions were studied as a control including Ag^+, Hg^{2+}, Cu^{2+}, Pb^{2+}, Co^{2+}, Fe^{2+}, Cr^{3+}, Mn^{2+}, Al^{3+}, Zr^{4+}, Ca^{2+}, Eu^{3+} and Ni^{2+}. As shown in Fig. 3b, most metal ions caused only slight influence on the fluorescence intensity at the concentration of 5 μM.

Analysis of Cd(II) in real samples

The turn-on fluorescence probe has been applied to Cd(II) analysis in real samples to evaluate its practicality. The samples were pre-treated according to the procedure described in **Section** "**Pre-treatment of Real samples**". Then, 100 μL real samples were added into the solution containing 200 μL N,P-CDs and 100 μL HAc-NaAc buffer (10 mM, pH 6.0), and then diluted to 2 mL with ultrapure water. The measurement were carried out after incubating for 15 min with excitation/emission peaks at 325/435 nm. A recovery experiment was also carried out with spiking different concentrations of Cd(II) into the real samples. As shown in Table 1, the found values

Fig. 3 a FTIR spectra of N,P-CDs without and with the addition of Cd(II); **b** Selectivity towards Cd(II) over the other metal ions with the metal ion concentration of 5 μM. Experimental conditions: The total 2 mL solution consisted of 200 μL N,P-CDs, 10 μL 1 mM of different metal ions and 100 μL acetate buffer (pH 6.0) reacting for 15 min at room temperature
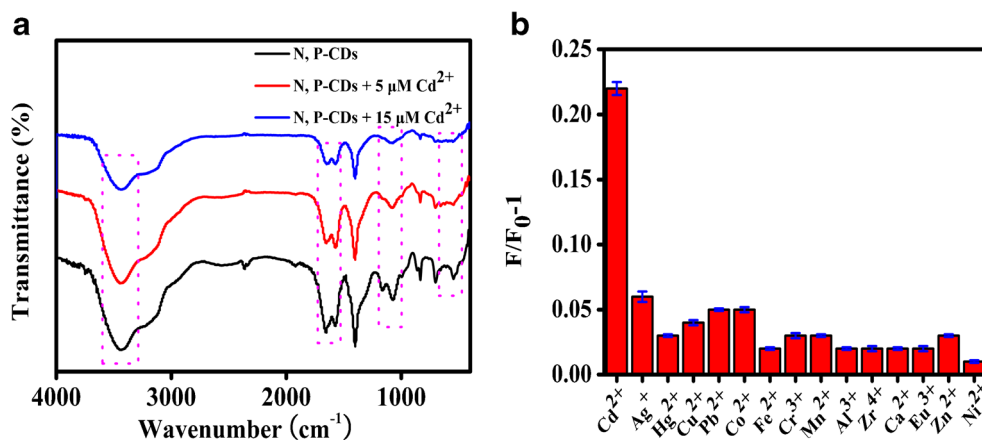
Table 1 Detection of Cd(II) in real samples with the turn-on fluorescence probe ($n = 3$)

Samples	Add (µM)	Found (µM)	Recovery (%)	R.S.D. (%)
Serum sample 1	5	4.5	90	4.7
Serum sample 2	10	10.4	104	4.6
Urine sample 1	5	5.2	104	4.5
Urine sample 2	7.5	7.2	96	3.8

agreed with the addition of Cd(II). The recoveries ranged from 90% to 104% with the relative standard deviations (R.S.D.) of three replicate detections for each sample below 5%. These results confirmed the practicality for the turn-on fluorescence probe for the detection of Cd(II) in real samples.

Conclusions

Highly photoluminescent N,P-CDs have been synthesized via hydrothermal method with CA and PEA as sources. The N,P-CDs exhibited excellent optical properties and were used as a turn-on fluorescence probe for the detection of Cd(II) with a detection limit of 0.16 µM. The fluorescence enhancement on addition of Cd(II) was attributed to the formation of Cd(II)-N,P-CDs complex via the chelation between Cd(II) with functional groups on the surface. As far as we know, this is the first report utilizing N,P-CDs as a turn-on fluorescence probe for Cd(II) detection based on CHEF mechanism. Additionally, the results for Cd(II) detection in real samples promised the great application of N,P-CDs based turn-on fluorescence probe in health and environmental protection.

Compliance with ethical standards The author(s) declare that they have no competing interests.

Publisher's note Springer Nature remains neutral with regard to jurisdictional claims in published maps and institutional affiliations.

References

1. Agency for Toxic Substances and Disease Registry (2017) Substance Priority List, Atlanta, GA 30341. https://www.atsdr.cdc.gov/spl/index.html#2017spl . Accessed 10 Aug 2017

2. Peng XJ, Du JJ, Fan J et al (2007) A selective fluorescent sensor for imaging Cd^{2+} in living cells. J Am Chem Soc 129:1500–1501. https://doi.org/10.1021/ja0643319

3. Mahajan PG, Bhopate DP, Koleka GB et al (2015) N-methyl isatin nanoparticles as a novel probe for selective detection of Cd^{2+} ion in aqueous medium based on chelation enhanced fluorescence and applications to environmental sample. Sensors Actuators B Chem 220:864–872. https://doi.org/10.1016/j.snb.2015.05.119

4. Mameli M, Aragoni MC, Arca M et al (2010) A selective, nontoxic, off-on fluorescent molecular sensor based on 8-hydroxyquinoline for probing Cd^{2+} in living cells. Chem Eur J 16:919–930. https://doi.org/10.1002/chem.200902005

5. Gui RJ, An XQ, Su HJ et al (2012) A near-infrared-emitting CdTe/CdS core/shell quantum dots-based off-on fluorescence sensor for highly selective and sensitive detection of Cd^{2+}. Talanta 94:257–262. https://doi.org/10.1016/j.talanta.2012.03.036

6. Wang ZX, Guo YX, Ding SN (2015) Fluorometric determination of cadmium(II) and mercury(II) using nanoclusters consisting of a gold-nickel alloy. Microchim Acta 182:2223–2231. https://doi.org/10.1007/s00604-015-1563-z

7. Zu FL, Yan FY, Bai ZJ et al (2017) The quenching of the fluorescence of carbon dots: a review on mechanisms and applications. Microchim Acta 184:1899–1914. https://doi.org/10.1007/s00604-017-2318-9

8. Gao XH, Du C, Zhuang ZH et al (2016) Carbon quantum dot-based nanoprobes for metal ion detection. J Mater Chem C 4:6927–6945. https://doi.org/10.1039/C6TC02055K

9. Zhang J, Yu SH (2016) Carbon dots: large-scale synthesis, sensing and bioimaging. Mater Today 19:382–393. https://doi.org/10.1016/j.mattod.2015.11.008

10. Du Y, Guo SJ (2016) Chemically doped fluorescent carbon and graphene quantum dots for bioimaging, sensor, catalytic and photoelectronic applications. Nanoscale 8:2532–2543. https://doi.org/10.1039/C5NR07579C

11. Xu Q, Kuang TR, Liu Y et al (2016) Heteroatom-doped carbon dots: synthesis, characterization, properties, photoluminescence mechanism and biological applications. J Mater Chem B 4:7204–7219. https://doi.org/10.1039/C6TB02131J

12. Lin LP, Song XH, Chen YY et al (2015) Intrinsic peroxidase-like catalytic activity of nitrogen-doped graphene quantum dots and their application in the colorimetric detection of H_2O_2 and glucose. Anal Chim Acta 869:89–95. https://doi.org/10.1016/j.aca.2015.02.024

13. Yang F, He X, Wang CX et al (2018) Controllable and eco-friendly synthesis of P-riched carbon quantum dots and its application for copper (II) ion sensing. Appl Surf Sci 448:589–598. https://doi.org/10.1016/j.apsusc.2018.03.246

14. Guo YM, Cao FP, Li YB (2018) Solid phase synthesis of nitrogen and phosphor co-doped carbon quantum dots for sensing Fe^{3+} and the enhanced photocatalytic degradation of dyes. Sensors Actuators B Chem 255:1105–1111. https://doi.org/10.1016/j.snb.2017.08.104

15. Li H, Shao FQ, Zou SY et al (2015) Microwave-assisted synthesis of N, P-doped carbon dots for fluorescent cell imaging. Microchim Acta 183:821–826. https://doi.org/10.1016/j.apsusc.2018.03.246

16. Ananthanarayanan A, Wang Y, Routh P et al (2015) Nitrogen and phosphorus co-doped graphene quantum dots: synthesis from adenosine triphosphate, optical properties, and cellular imaging. Nanoscale 7:8159–8165. https://doi.org/10.1039/c5nr01519g

17. Parvin N, Mandal TK (2017) Dually emissive P, N-co-doped carbon dots for fluorescent and photoacoustic tissue imaging in living mice. Microchim Acta 184:1117–1125. https://doi.org/10.1007/s00604-017-2108-4

18. Shi BF, Su YB, Zhang LL et al (2016) Nitrogen and phosphorus co-doped carbon nanodots as a novel fluorescent probe for highly sensitive detection of Fe^{3+} in human serum and living cells. ACS

Appl Mater Interfaces 8:10717–10725. https://doi.org/10.1021/acsami.6b01325

19. Li JJ, Jiao YZ, Feng LD, Zhong Y, Zuo G, Xie A, Dong W (2017) Highly N, P-doped carbon dots: rational design, photoluminescence and cellular imaging. Microchim Acta 184:2933–2940. https://doi.org/10.1007/s00604-017-2314-0

20. Du FF, Li G, Gong XJ et al (2018) Facile, rapid synthesis of N, P-dual-doped carbon dots as a label-free multifunctional nanosensor for Mn(VII) detection, temperature sensing and cellular imaging. Sensors Actuators B Chem 277:492–501. https://doi.org/10.1016/j.snb.2018.09.027

21. Li JC, Hou PX, Cheng M et al (2018) Carbon nanotube encapsulated in nitrogen and phosphorus co-doped carbon as a bifunctional electrocatalyst for oxygen reduction and evolution reactions. Carbon 139:156–163. https://doi.org/10.1016/j.carbon.2018.06.023

22. Gong YQ, Yu B, Yang W et al (2016) Phosphorus, and nitrogen co-doped carbon dots as a fluorescent probe for real-time measurement of reactive oxygen and nitrogen species inside macrophages. Biosens Bioelectron 79:822–828. https://doi.org/10.1016/j.bios.2016.01.022

23. Huang S, Yang EL, Liu Y et al (2018) Low-temperature rapid synthesis of nitrogen and phosphorus dual-doped carbon dots for multicolor cellular imaging and hemoglobin probing in human blood. Sensors Actuators B Chem 265:326–334. https://doi.org/10.1016/j.snb.2018.03.056

24. Chandra S, Laha D, Pramanik A et al (2016) Synthesis of highly fluorescent nitrogen and phosphorus doped carbon dots for the detection of Fe^{3+} ions in cancer cells. Luminescence 31:81–87. https://doi.org/10.1002/bio.2927

25. Yu CY, Xuan TT, Yan D et al (2017) Sesame-derived ions co-doped fluorescent carbon nanoparticles for bio-imaging, sensing and patterning applications. Sensors Actuators B Chem 253:900–910. https://doi.org/10.1016/j.snb.2017.07.043

26. Fu X, Sheng L, Yu YS et al (2018) Rapid and universal detection of ovalbumin based on N, O, P-co-doped carbon dots-fluorescence resonance energy transfer technology. Sensors Actuators B Chem 269:278–287. https://doi.org/10.1016/j.snb.2018.04.134

27. Liu Y, Gong XJ, Dong WJ et al (2018) Nitrogen and phosphorus dual-doped carbon dots as a label-free sensor for curcumin determination in real sample and cellular imaging. Talanta 183:61–69. https://doi.org/10.1016/j.talanta.2018.02.060

28. Gong XJ, Liu Y, Yang ZH et al (2017) An "on-off-on" fluorescent nanoprobe for recognition of chromium(VI) and ascorbic acid based on phosphorus/nitrogen dual-doped carbon quantum dot. Anal Chim Acta 968:85–96. https://doi.org/10.1016/j.aca.2017.02.038

29. Wang X, Cao L, Lu FS et al (2009) Photoinduced electron transfers with carbon dots. Chem Commun 0:3774–3776. https://doi.org/10.1039/B906252A

30. Bhamore JR, Jha S, Singhal RK et al (2018) Facile green synthesis of carbon dots from pyrus pyrifolia fruit for assaying of Al^{3+} ion via chelation enhanced fluorescence mechanism. J Mol Liq 264:9–16. https://doi.org/10.1016/j.molliq.2018.05.041

31. Dong YJ, Ding LL, Jin X et al (2017) Silver nanoparticles capped with chalcon carboxylic acid as a probe for colorimetric determination of cadmium(II). Microchim Acta 184:3357–3362. https://doi.org/10.1007/s00604-017-2358-1

32. Omer KM, Hassan AQ (2017) Chelation-enhanced fluorescence of phosphorus doped carbon nanodots for multi-ion detection. Microchim Acta 184:2063–2071. https://doi.org/10.1007/s00604-017-2196-1

33. Gao XH, Lu YZ, Zhang RR et al (2015) One-pot synthesis of carbon nanodots for fluorescence turn-on detection of ag$^+$ based on the ag$^+$-induced enhancement of fluorescence. J Mater Chem C 3:2302–2309. https://doi.org/10.1039/C4TC02582B

34. Chandra S, Pathan SH, Mitra S et al (2012) Tuning of photoluminescence on different surface functionalized carbon quantum dots. RSC Adv 2:3602–3606. https://doi.org/10.1039/C2RA00030J